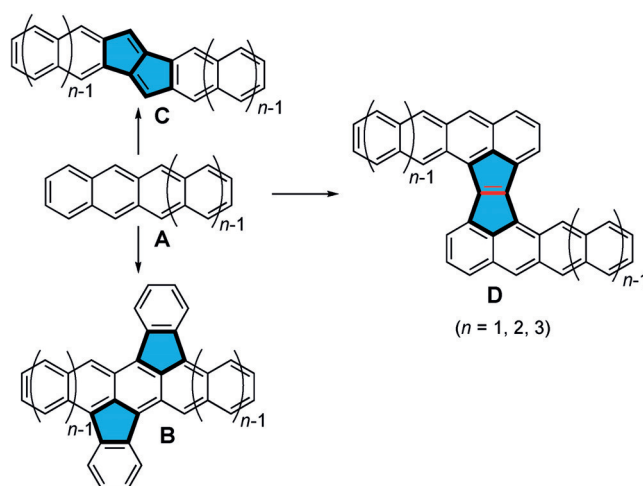


# Z-Shaped Pentaleno-Acene Dimers with High Stability and Small Band Gap

Gaole Dai, Jingjing Chang, Jie Luo, Shaoqiang Dong, Naoki Aratani, Bin Zheng, Kuo-Wei Huang, Hiroko Yamada, and Chunyan Chi\*

**Abstract:** Acene-based materials have promising applications for organic electronics but the major constrain comes from their poor stability. Herein a new strategy to stabilize reactive acenes, by fusion of an anti-aromatic pentalene unit onto the zigzag edges of two acene units to form a Z-shaped acene dimer, is introduced. The Z-shaped acene dimers are extremely stable and show a small energy gap resulting from intra-molecular donor–acceptor interactions. X-ray crystallographic analysis revealed their unique geometry and one-dimensional slip-stack columnar structure. Besides optical and electro-chemical characterizations, solution-processed field-effect transistors were also fabricated.

Acenes (**A**, Figure 1) have attracted a long-term interest because of their unique electronic structure and physical properties, and promising applications for organic electronics.<sup>[1]</sup> However, the intrinsic high reactivity arising from their high-lying HOMO energy levels limited their practical applications.<sup>[2]</sup> In recent years, different strategies have been developed to decrease the HOMO energy level and stable acenes, up to nonacene, are now accessible.<sup>[2–3]</sup> Incorporation of a five-membered ring into a polycyclic aromatic hydrocarbon framework has been demonstrated to be an efficient way to approach more-stable materials,<sup>[4]</sup> and this concept was recently extended to acene systems by us.<sup>[5]</sup> For example, we found that the fusion of two five-membered rings onto the zigzag edges of acene molecules resulted in very stable acenes having a small band gap (**B**) as a result of an intramolecular donor–acceptor interaction, as well as kinetic blocking of the reactive zigzag edges.<sup>[5a]</sup> Alternatively, fusion of an anti-aromatic pentalene unit along the long axis of an acene (**C**) is another way to approach making stable acene-based materials for applications such as ambipolar organic field effect



**Figure 1.** Three strategies towards stable five-membered ring fused acenes.

transistors (OFETs).<sup>[5b–c,6]</sup> However, we believe that a more efficient way for stabilization is to fuse the pentalene unit to the zigzag edges of acene molecules because the HOMO coefficients of acenes mainly localize at the zigzag edges, and thus we hypothesized that Z-shaped pentaleno-acene dimers (**D**) would be stable and show dramatically different properties from their respective acene monomers. In addition, the dimers could have a “fixed” double bond between the five-membered rings, and would thus be different from any other reported  $\pi$ -conjugated acene dimers.<sup>[7]</sup> In this context, herein we report our synthetic efforts towards these types of interesting but challenging molecules, their unique electronic and optical properties, their ground-state geometry, and their potential applications for OFETs.

The synthesis of the parent pentaleno-anthracene dimer **D**, ( $n = 1$ ; Figure 1) was attempted by Clar but failed because of the poor stability and solubility of the product.<sup>[8]</sup> Therefore, in our design, bulky trialkylsilyl ethynyl substituents are strategically attached to outer zigzag edges to ensure sufficient solubility and stability (Scheme 1). The key intermediates towards the target pentaleno-anthracene **1** and tetracene dimer **2a,b** are the corresponding quinones **7** and **11**. Our main synthetic strategy involved the synthesis of a dibenzopentalene intermediate, carrying two aryl ester substituents, by a palladium-catalyzed cyclodimerization reaction<sup>[9]</sup> followed by hydrolysis and a regioselective Friedel–Crafts acylation reaction. Sonogashira coupling between 1-bromo-2-ethynylbenzene (**3**) and methyl 2-iodobenzoate (**4**) gave the *ortho*-bromo tolane derivative. Then  $[\text{Pd}_2(\text{dba})_3]$ -catalyzed cyclodimerization of **5** provided the dibenzopentalene diester

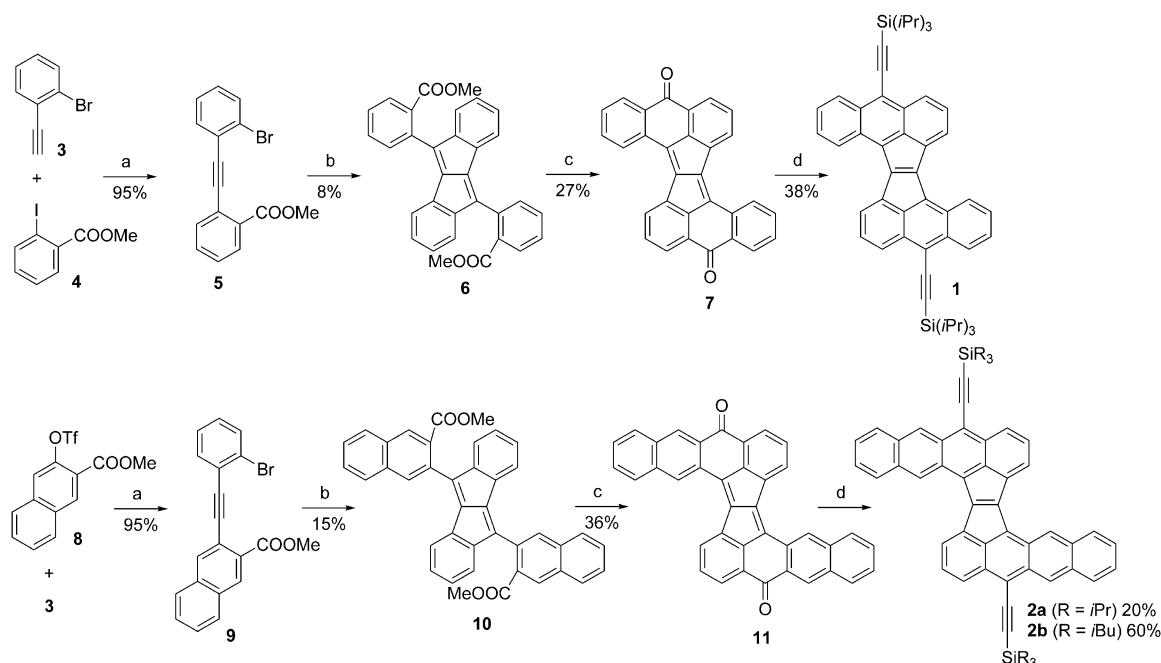
\*] Dr. G. Dai, Dr. J. Chang, Dr. S. Dong, Prof. C. Chi  
Department of Chemistry, National University of Singapore  
3 Science Drive 3, 117543 (Singapore)  
E-mail: chmcc@nus.edu.sg

Dr. J. Luo  
Institute of Materials Research and Engineering, A\*STAR  
3 Research Link, 117602 (Singapore)

Prof. N. Aratani, Prof. H. Yamada  
Graduate School of Materials Science, Nara Institute of Science and Technology (NAIST), Ikoma 630-0192 (Japan)

Dr. B. Zheng, Prof. K.-W. Huang  
KAUST Catalysis Center and Division of Physical Sciences & Engineering, King Abdullah University of Science and Technology (KAUST), Thuwal 23955-6900 (Saudi Arabia)

Supporting information for this article is available on the WWW under <http://dx.doi.org/10.1002/anie.201508919>.



**Scheme 1.** Reagents and conditions: a)  $[\text{Pd}(\text{PPh}_3)_2\text{Cl}_2]$ , CuI,  $\text{Et}_3\text{N}/\text{THF}$  (or DMF), RT; b)  $[\text{Pd}_2(\text{dba})_3]$ ,  $\text{P}(2\text{-furyl})_3$ ,  $\text{Cs}_2\text{CO}_3$ , CsF, hydroquinone, 1,4-dioxane,  $135^\circ\text{C}$ ; c) 1. LiOH, dioxane/ $\text{H}_2\text{O}$ , reflux; 2.  $\text{SOCl}_2$ , DCM; 3.  $\text{AlCl}_3$ , DCM, RT; d) 1.  $\text{R}_3\text{SiCCl}_2$ , THF; 2.  $\text{SnCl}_2$ , HCl (aq.) dba = dibenzylideneacetone, DCM = dichloromethane, DMF = *N,N*-dimethylformamide, THF = tetrahydrofuran.

**6.** The ester groups in **6** were hydrolyzed to give the diacid and then converted into the acyl chloride by reaction with thionyl chloride. Subsequent  $\text{AlCl}_3$ -catalyzed intramolecular Friedel–Crafts acylation selectively afforded the desired pentaleno-bis(anthracenequinone) **7** rather than an isomer containing a seven-membered ring. Nucleophilic addition of **7** with triisopropylsilyl ethynyl (TIPS) lithium and subsequent reduction of the resulting diol with  $\text{SnCl}_2$  gave the target **1**. Following a similar strategy, the pentaleno-bis(tetracenequinone) **11** was obtained from **8**<sup>[10]</sup> and **3**. The TIPS-substituted tetracene dimer **2a** was obtained but it has poor solubility, thus more bulky triisobutylsilyl ethynyl (TIBS) groups were introduced. The obtained dimer **2b** has good solubility in common organic solvents such as THF, chloroform, and toluene. Similarly, starting from an anthracene analogue of **5** and **9**, a pentaleno-bis(pentacenequinone) **19** was also synthesized (see Scheme S1 in the Supporting Information). However, the subsequent nucleophilic addition reactions with various trialkylsilyl ethynyl lithium (or magnesium bromide) and reduction all failed to give any desired pentacene dimers because of the poor solubility of the quinone. Anyway, the soluble and stable **1** and **2b** allowed full characterizations and comparisons with the respective monomers and other types of dimers.

The compound **1** displays a purple-pink color in THF and shows a distinctively different UV-vis-NIR absorption spectrum (Figure 2a) from that of the 9,10-bis-TIPS-substituted anthracene monomer (TIPS-Anthracene; see Figure S1a). In addition to a well-resolved band with three peaks at  $\lambda = 490$ , 526, and 567 nm (band II), similar to the p-band of acenes (Figure 2a), a broad band with three peaks at  $\lambda = 694$ , 750, and 831 nm (band I) is observed, and it is significantly red-shifted compared to that of the pentalene-bridged anthracene dimer analogue (**C**,  $n=3$ , see derivative DAP1 with the

longest absorption maximum wavelength  $\lambda_{\text{max}} = 556$  nm, Figure S1a).<sup>[5b]</sup> An intense absorption band (band III) at short wavelength (250–400 nm,  $\lambda_{\text{max}} = 252$  nm) was also observed. Time-dependent density functional theory (TDDFT) calculations (B3LYP/6-31G\*; see the Supporting Information for details) indicate that band I originated from the HOMO  $\rightarrow$  LUMO transition ( $\lambda = 816.5$  nm, oscillator strength  $f = 0.2554$ ), while band II mainly comes from the HOMO-1  $\rightarrow$  LUMO transition ( $\lambda = 567.8$  nm,  $f = 0.4741$ ). Band III is a combination of multiple HOMO- $n \rightarrow$  LUMO +  $m$  transitions. Interestingly, calculations also show that both the HOMO and LUMO of **1** are delocalized along the Z-shaped  $\pi$ -conjugated framework while the distribution is different with some disjointed features (Figure 3), thus indicating an intramolecular donor–acceptor interaction which can be correlated to the broad absorption at long-wavelength (Figure 2a).

The compound **2b** displays a green color in THF and its absorption spectrum is different from that of the 5,12-bis-TIPS-substituted tetracene monomer (TIPS-Tetracene) but similar to that of **1**, with a significant red-shift of each band because of the extended  $\pi$ -conjugation (Figure 2; see Figure S1b). In particular, the shoulder of the longest-wavelength absorption band (band I) is red-shifted by 155 nm, and bands II and III are red-shifted by 98 and 33 nm, respectively. The characteristics of these bands are similar to those for **1**, HOMO  $\rightarrow$  LUMO transition ( $\lambda = 1009.7$  nm,  $f = 0.3197$ ) for band I and HOMO-2  $\rightarrow$  LUMO transition ( $\lambda = 655.7$  nm,  $f = 0.2354$ ) for band II. The optical energy gap ( $E_g^{\text{opt}}$ ) was determined as 1.41 and 1.17 eV for **1** and **2b**, respectively. In addition, UV-vis-NIR absorption spectral measurements in various solvents with different polarity did not show obvious changes (see Figure S2), thus indicating a negligible intramolecular charge-transfer character.

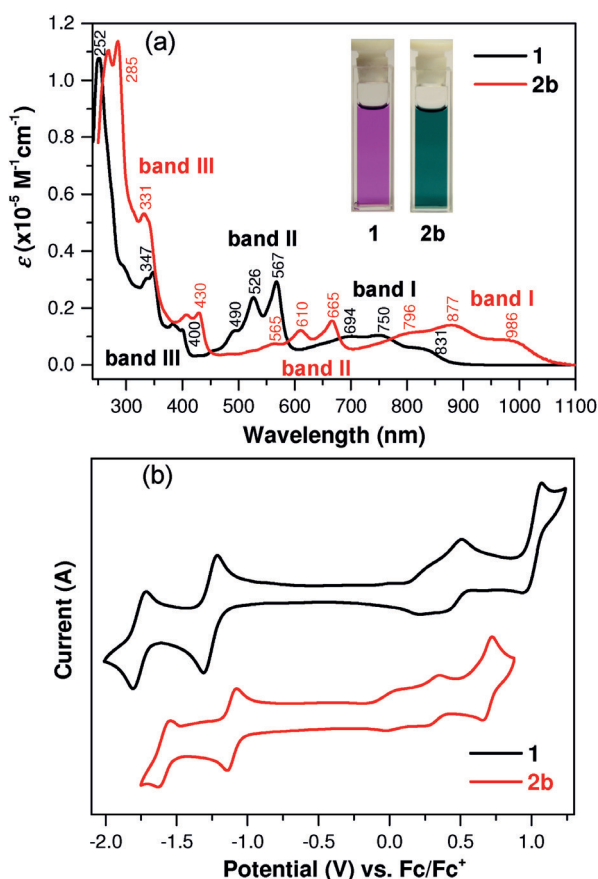


**Figure 2.** a) UV-vis-NIR absorption spectra of **1** and **2b** recorded in THF ( $1 \times 10^{-5}$  M). Insert: photos of the solutions. b) Cyclic voltammograms of **1** and **2b** in DCM with 0.1 M  $\text{Bu}_4\text{NPF}_6$  as the supporting electrolyte, Ag/AgCl as the reference electrode, Pt wire as the counter electrode, and a scan rate at  $50 \text{ mV s}^{-1}$ . The electrode potential was externally calibrated by  $\text{Fc}^+/\text{Fc}$  couple.

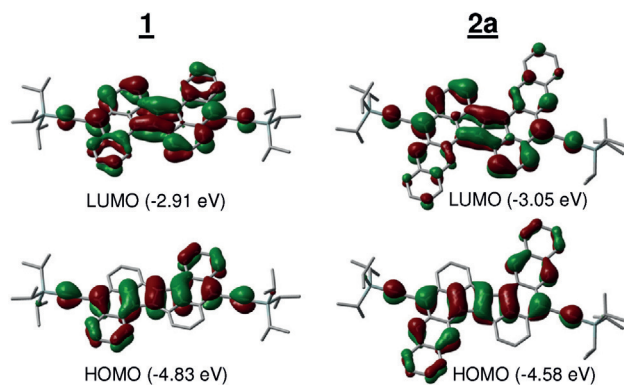


**Figure 3.** Calculated (B3LYP/6-31G\*) frontier molecular orbital profiles and energy levels of **1** and **2a**.

Cyclic voltammetry (CV) and differential pulse voltammetry (DPV) were used to study the electrochemical properties of **1** and **2b** in dry dichloromethane (DCM; Figure 2b; see Figure S7). Three quasi-reversible oxidation waves with half-wave potentials  $E_{1/2}^{\text{ox}}$  at 0.22, 0.44, and 1.00 V and two reversible reduction waves with half-wave potentials  $E_{1/2}^{\text{red}}$  at  $-1.27$  and  $-1.78$  V (vs.  $\text{Fc}^+/\text{Fc}$ ,  $\text{Fc}$ : ferrocene) were observed for **1**. **2b** showed three quasi-reversible oxidation waves with  $E_{1/2}^{\text{ox}}$

at 0.01, 0.29, and 0.67 V, and two reversible reduction waves with  $E_{1/2}^{\text{red}}$  at  $-1.13$  and  $-1.61$  V. The HOMO/LUMO energy levels are determined to be  $-4.95/-3.62$  and  $-4.69/-3.75$  eV for **1** and **2b**, respectively, from the onset of the first oxidation/reduction wave. The corresponding electrochemical energy gaps ( $E_g^{\text{EC}}$ ) were then estimated to be 1.33 eV for **1** and 0.94 eV for **2b**, and are consistent with their optical energy band gaps.

The photo-oxidative decay of **1** and **2b**, and their monomer counter parts TIPS-Anthracene and TIPS-Tetracene, was monitored by UV-vis absorption spectroscopy in THF solutions ( $2 \times 10^{-5}$  M) under the same ambient light and air conditions (see Figure S8). TIPS-Anthracene and TIPS-Tetracene solutions are stable with a half-life time ( $t_{1/2}$ ) of 344 and 195 h, respectively. The compounds **1** and **2b** both exhibited high photostability, with a  $t_{1/2}$  of 221 h for **1** and 54 days for **2b**, which are also much more stable than the perfused anthracene dimer [bis(anthene)]<sup>[7a]</sup> and tetracene dimer [bis(tetracene)] analogues.<sup>[7d]</sup> The largely enhanced photostability of **1** and **2b** can be ascribed to: 1) the introduction of an electron-deficient pentalene unit dramatically lowers the HOMO energy levels in comparison to the perfused bis(anthene) and peritetracene (see Figure S3); and 2) kinetic stabilization by the TIPS groups<sup>[11]</sup> and the five-membered rings at the zigzag edge.

Single crystals of **1** and **2b** suitable for X-ray crystallographic analysis were obtained by slow diffusion of either methanol or acetonitrile into a THF solution.<sup>[12]</sup> Both **1** and **2b** have a rigid planar  $\pi$ -conjugated skeleton (Figure 4). The central carbon-carbon bond between the two five-membered rings in **1** has a bond length of 1.384 Å, thus indicating a significant double-bond character as predicted. The size and quality of the single crystals of **2b** were not good enough to allow us to do an accurate bond length analysis. Interestingly, both molecules show a slip-stack columnar structure through close  $\pi$ - $\pi$  interactions [3.294(6) Å in **1** and 3.271(4) Å in **2b**] and the neighboring molecules in the column adopt an alternating orthogonal arrangement to suppress steric repulsion between the bulky substituents.

Considering the ordered packing, OFETs of **1** and **2b** were fabricated by solution processed thin films using a bottom-gate top-contact device structure, and all devices measured in  $\text{N}_2$  exhibited p-type behavior (see Figure S9). Under optimal reaction conditions, a hole mobility ( $\mu_h$ ) of  $6.0 \times 10^{-3} \text{ cm}^2 \text{ V}^{-1} \text{ s}^{-1}$ , threshold voltage ( $V_T$ ) of  $-4$  V, and current on/off ratio ( $I_{\text{on}}/I_{\text{off}}$ ) of  $6 \times 10^5$  were achieved for **1**. The relatively low performance can be ascribed to the weak crystalline nature and much grain boundaries exist for the solution-processed thin films as revealed by X-ray diffraction and atomic force microscope measurements (see Figures S10 and S11). The devices of **2b** gave comparable performance ( $\mu_h$ :  $1.7 \times 10^{-3} \text{ cm}^2 \text{ V}^{-1} \text{ s}^{-1}$ ,  $V_T$ :  $-2$  V,  $I_{\text{on}}/I_{\text{off}}$ :  $10^3$ ) for similar reasons. The device performance of both molecules could be further improved by using vapour-deposited thin films or single crystals in the future.

In summary, Z-shaped, the pentaleno-acene dimers **1** and **2a,b** were designed and synthesized. It was found that the fusion of an anti-aromatic pentalene moiety to the zigzag edges of acenes dramatically changed their ground-state electronic structure and physical properties. As a result of the



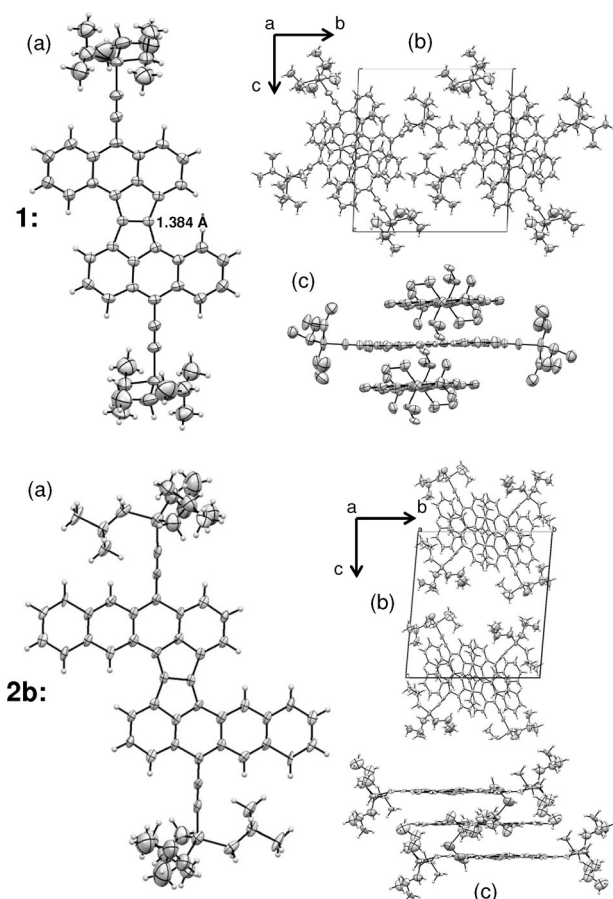


**Figure 4.** X-ray crystallographic structures and three-dimensional packing of **1** and **2b**: a) ORTEP drawing; b) packing along the *a*-axis (top view); c) side view. Thermal ellipsoids shown at 30% probability.

intramolecular donor–acceptor interaction, both compounds show very small band gaps and amphoteric redox behavior. Stable materials were obtained because of both thermodynamic stabilization and kinetic blocking. Our study demonstrates a new strategy to approach stable acenes, heteroacenes, and perifused acenes in the future.

## Acknowledgments

C.C. acknowledges financial support from the MOE Tier 1 grant (R-143-000-573-112), Tier 2 grant (MOE2014-T2-1-080), and Tier 3 programme (MOE2014-T3-1-004). K.-W.H. acknowledges financial support from KAUST.

**Keywords:** acenes · dimerization · materials science · polycycles · structure elucidation

**How to cite:** *Angew. Chem. Int. Ed.* **2016**, *55*, 2693–2696  
*Angew. Chem.* **2016**, *128*, 2743–2746

- [1] a) M. Bendikov, F. Wudl, D. F. Perepichka, *Chem. Rev.* **2004**, *104*, 4891; b) J. E. Anthony, *Chem. Rev.* **2006**, *106*, 5028; c) J. E. Anthony, *Angew. Chem. Int. Ed.* **2008**, *47*, 452; *Angew. Chem.* **2008**, *120*, 460; d) H. Qu, C. Chi, *Curr. Org. Chem.* **2010**, *14*, 2070; e) Z. Sun, Q. Ye, C. Chi, J. Wu, *Chem. Soc. Rev.* **2012**, *41*, 7857; f) Q. Ye, C. Chi, *Chem. Mater.* **2014**, *26*, 4046.

- [2] a) O. Berg, E. L. Chronister, T. Yamashita, G. W. Scott, R. M. Sweet, J. Calabrese, *J. Phys. Chem. A* **1999**, *103*, 2451; b) I. Kaur, W. Jia, R. P. Kopreski, S. Selvarasah, R. Dokmeci, C. Pramanik, N. E. Mcgruer, G. P. Miller, *J. Am. Chem. Soc.* **2008**, *130*, 16274; c) B. Purushothaman, S. R. Parkin, J. E. Anthony, *Org. Lett.* **2010**, *12*, 2060; d) B. Purushothaman, M. Bruzek, S. R. Parkin, A. F. Miller, J. E. Anthony, *Angew. Chem. Int. Ed.* **2011**, *50*, 7013; *Angew. Chem.* **2011**, *123*, 7151.
- [3] a) J. E. Anthony, D. L. Eaton, S. R. Parkin, *Org. Lett.* **2002**, *4*, 15; b) Y. Sakamoto, T. Suzuki, M. Kobayashi, Y. Gao, Y. Fukai, Y. Inoue, F. Sato, S. Tokito, *J. Am. Chem. Soc.* **2004**, *126*, 8138; c) D. Chun, Y. Cheng, F. Wudl, *Angew. Chem. Int. Ed.* **2008**, *47*, 8380; *Angew. Chem.* **2008**, *120*, 8508; d) H. Qu, C. Chi, *Org. Lett.* **2010**, *12*, 3360; e) H. Qu, W. B. Cui, J. Li, J. Shao, C. Chi, *Org. Lett.* **2011**, *13*, 924; f) Q. Ye, J. Chang, K.-W. Huang, C. Chi, *Org. Lett.* **2011**, *13*, 5960; g) S. Katsuta, K. Tanaka, Y. Maruya, S. Mori, S. Masuo, T. Okujima, H. Uno, K.-I. Nakayama, H. Yamada, *Chem. Commun.* **2011**, *47*, 10112; h) W. Fudickar, T. Linker, *J. Am. Chem. Soc.* **2012**, *134*, 15071; i) U. H. F. Bunz, J. U. Engelhart, B. D. Lindner, M. Schaffroth, *Angew. Chem. Int. Ed.* **2013**, *52*, 3810; *Angew. Chem.* **2013**, *125*, 3898.
- [4] a) M. Smet, R. Shukla, L. Fülöp, W. Dehaen, *Eur. J. Org. Chem.* **1998**, 2769; b) A. R. Mohebbi, J. Yuen, J. Fan, C. Munoz, M. Wang, R. S. Shirazi, J. Seifert, F. Wudl, *Adv. Mater.* **2011**, *23*, 4644; c) C. Lütke Eversloh, Y. Avlasevich, C. Li, K. Müllen, *Chem. Eur. J.* **2011**, *17*, 12756; d) J. D. Wood, J. L. Jellison, A. D. Finke, L. Wang, K. N. Plunkett, *J. Am. Chem. Soc.* **2012**, *134*, 15783; e) H. Xia, D. Liu, X. Xu, Q. Miao, *Chem. Commun.* **2013**, *49*, 4301.
- [5] a) A. Naibi Lakshminarayana, J. Chang, J. Luo, B. Zheng, K.-W. Huang, C. Chi, *Chem. Commun.* **2015**, *51*, 3604; b) G. Dai, J. Chang, W. Zhang, S. Bai, K.-W. Huang, J. Xu, C. Chi, *Chem. Commun.* **2015**, *51*, 503; c) G. Dai, J. Chang, X. Shi, W. Zhang, B. Zheng, K.-W. Huang, C. Chi, *Chem. Eur. J.* **2015**, *21*, 2019.
- [6] a) T. Kawase, T. Fujiwara, C. Kitamura, A. Konishi, Y. Hirao, K. Matsumoto, H. Kurata, T. Kubo, S. Shinamura, H. Mori, E. Miyazaki, K. Takimiya, *Angew. Chem. Int. Ed.* **2010**, *49*, 7728; *Angew. Chem.* **2010**, *122*, 7894; b) M. Nakano, I. Osaka, K. Takimiya, T. Koganezawac, *J. Mater. Chem. C* **2014**, *2*, 64.
- [7] a) J. Li, K. Zhang, X. Zhang, K. Huang, C. Chi, J. Wu, *J. Org. Chem.* **2010**, *75*, 856; b) X. Zhang, X. Jiang, J. Luo, C. Chi, H. Chen, J. Wu, *Chem. Eur. J.* **2010**, *16*, 464; c) L. Zhang, A. Fonari, Y. Liu, A.-L. Hoyt, H. Lee, D. Granger, S. Parkin, T. P. Russell, J. E. Anthony, J.-L. Bredas, V. Coropceanu, A. L. Briseno, *J. Am. Chem. Soc.* **2014**, *136*, 9248; d) J. Liu, P. Ravat, M. Wagner, M. Baumgarten, X. Feng, K. Müllen, *Angew. Chem. Int. Ed.* **2015**, *54*, 12442; *Angew. Chem.* **2015**, *127*, 12619.
- [8] E. Clar, *Ber. Dtsch. Chem. Ges.* **1939**, *72*, 2134.
- [9] a) T. Kawase, A. Konishi, Y. Hirao, K. Matsumoto, H. Kurata, T. Kubo, *Chem. Eur. J.* **2009**, *15*, 2653; b) Z. U. Levi, T. D. Tilley, *J. Am. Chem. Soc.* **2009**, *131*, 2796.
- [10] a) K. Mori, T. Kawasaki, T. Akiyama, *Org. Lett.* **2012**, *14*, 1436; b) Z. Huang, Z. Liu, J. Zhou, *J. Am. Chem. Soc.* **2011**, *133*, 15882.
- [11] a) A. Maliakal, K. Raghavachari, H. Katz, E. Chandross, T. Siegrist, *Chem. Mater.* **2004**, *16*, 4980; b) M. M. Payne, S. R. Parkin, J. E. Anthony, *J. Am. Chem. Soc.* **2005**, *127*, 8028; c) O. L. Griffith, J. E. Anthony, A. G. Jones, Y. Shu, D. L. Lichtenberger, *J. Am. Chem. Soc.* **2012**, *134*, 14185.
- [12] CCDC 1055934 (**1**) and 1055935 (**2b**) contain the supplementary crystallographic data for this paper. These data can be obtained free of charge from The Cambridge Crystallographic Data Centre.

Received: September 23, 2015

Revised: November 30, 2015

Published online: January 25, 2016